

Cite this article as: Wu Qingjie, Guo Zhenghua, Huang Qin, et al. Effect of AlCoCrFeNi High-Entropy Alloy on Microstructure and Mechanical Properties of Al-Si-Cu Alloy[J]. Rare Metal Materials and Engineering, 2024, 53(11): 3017-3025. DOI: 10.12442/j.issn.1002-185X.20240073.

ARTICLE

Effect of AlCoCrFeNi High-Entropy Alloy on Microstructure and Mechanical Properties of Al-Si-Cu Alloy

Wu Qingjie¹, Guo Zhenghua¹, Huang Qin², Lingli Shibao³

¹School of Aeronautic Manufacturing Engineering, Nanchang Hangkong University, Nanchang 330036, China; ²Technology R&D Department, Jiangxi Isuzu Motors Co., Ltd, Nanchang 330010, China; ³Jiashan Xinhai Precision Casting Co., Ltd, Jiaying 314101, China

Abstract: High-entropy alloy (HEA), as a class of new alloy materials characterized by high stability, excellent specific strength and corrosion resistance, has attracted much attention in the field of aluminum matrix composites (AMCs). To study the effect on microstructure and mechanical properties of aluminum alloys, AlCoCrFeNi HEA particles reinforced ADC12 composites were fabricated by high energy ultrasonic casting process. Subsequently, the effect of HEAs addition on the microstructure and mechanical properties of ADC12 alloys was investigated. Results show that the added HEA particles are tightly bonded to the aluminum matrix. The Al₂Cu phase in the matrix is refined. Meanwhile, the tensile strength and microhardness of the alloys with the addition of HEA particles are significantly improved. The yield strength and ultimate tensile strength of as-prepared composites with 12wt% HEAs are increased by 16.9% and 21.9% compared with those of the matrix, respectively. The wear rate of the composites is also decreased due to the enhancement of microhardness under applied load of 20 N. It is mainly attributed to the load transfer strengthening, dislocation proliferation and the optimization of the microstructure.

Key words: high-entropy alloy (HEA); ADC12 alloy; aluminum matrix composites (AMCs); mechanical properties

Aluminum matrix composite (AMC), an important component of metal matrix composite, has replaced single types of alloys in a variety of structural and other applications due to its enhanced properties such as high specific strength as well as excellent mechanical and tribological properties^[1-5]. To improve the mechanical properties of AMCs, ceramic particles, traditional metal particles or amorphous alloy particles (such as Al₂O₃, B₄C, Zr particles and Ni₆₀Nb₄₀) can be used to enhance mechanical properties^[6-11]. Prasad et al^[12] revealed that the hardness of the hybrid composite increased with increasing the volume fraction of reinforcement particles and the tensile properties increased with increasing the mass fraction of the reinforcement particles. Enel et al^[13] studied the effect of mixed binary graphene nanoplatelets and Al₂O₃ on the properties of aluminum matrix and found that the binary graphene nanoplatelets and Al₂O₃ create a synergic effect on the mechanical strength of composites, and effectively enhance the compressive capacity of the composites. Mordyuk et al^[14] used Al-Cu-Fe particles on the surface of Al-

Mg alloys to reinforce the Al-Mg matrix composite surface layer, and found that it can significantly improve the fatigue performance and wear resistance of the alloys. It has been shown that improving the performance of aluminum alloys by adding ceramic or metal particles is an effective approach. However, the disadvantages are obvious, i.e. the interfacial bonding of the ceramic to the aluminum alloy matrix is relatively poor. This seriously weakens load-bearing transfer between the reinforcement and the metal in tension or compression^[15]. Amorphous metal particles bond better with the matrix compared to ceramic particles. However, problems such as poor hardness and brittleness severely restrict their application^[16-17].

Recently, the application of high-entropy alloy (HEA) particles in composites has attracted much attention because HEAs, as a new type of metallic material, not only have natural metallic properties, but also possess physicochemical characteristics such as high strength, high hardness, high stability, and good abrasion and corrosion resistance^[18-19].

Received date: February 06, 2024

Foundation item: Science and Technology Research Program of Jiangxi Provincial Department of Education (GJJ190531)

Corresponding author: Huang Qin, Senior Engineer, Technology R&D Research and Development Department, Jiangxi Isuzu Motors Co., Ltd, Nanchang 330010,

E-mail: huang.qin@jiangxi-isuzu.cn

Copyright © 2024, Northwest Institute for Nonferrous Metal Research. Published by Science Press. All rights reserved.

HEAs do not have the disadvantage of poor wettability with the aluminum matrix and maintain excellent strength properties compared with ceramics or carbon materials. Preliminary work has been carried out to study HEAs as reinforcements for composites. Wang et al.^[20] used FeNiCrCoAl particles in 2024Al matrix composites by microwave low temperature sintering. The compressive strength of the fabricated composites was increased to 248.7 MPa. Liu^[21] studied the diffusion layer width of AlCoCrFeNi HEAs in the matrix and the strength of the prepared composites. There are many similar reports on the use of HEAs in composites^[22-23]. These literatures express the truth that HEAs are the better choice for reinforcement of AMCs due to their slow diffusion behavior and interfacial fusibility with the metal matrix compared with ceramic particles.

As we know, ADC12 aluminum alloy with good weldability, fluidity and filler-forming properties is widely used in the fields of rail transportation, energy construction and aerospace and aviation. With the rapid development of science and technology, aluminum alloys such as ADC12 with high strength, plasticity and wear resistance are strongly demanded in industrialization^[24-28]. The development of new lightweight and high-performance aluminum alloys has become an inevitable trend of development^[28-29]. Therefore, composites of AlCoCrFeNi HEA particle-reinforced ADC12 alloy were fabricated by high-energy ultrasonic casting process in this research. The effect of AlCoCrFeNi HEA particle on the morphology was assessed as well as its impact on mechanical properties of as-cast ADC12 alloy. Meanwhile, the interface as well as the strengthening mechanism of HEA/ADC12 composites in tension or compression was also studied^[15].

1 Experiment

The HEAs used in this research with an average particle diameter of 44.81 μm were provided by Hunan Tianjiu Co., Ltd and prepared by mechanical alloying. Five pure metal powders (purity \geq 99.9%, particle size \leq 50 μm) of Al, Cr, Fe, Ni and Co were used to prepare the particles by mechanical ball milling in argon atmosphere at a speed of 200 r/min. Fig. 1a shows a typical spherical microstructure of the micron-sized AlCoCrFeNi HEAs obtained by a field emission scanning electron microscope (SEM, Quanta200F EDAX). Correspondingly, Fig. 1b exhibits the energy dispersive spectrometer (EDS) elemental line scan results along red line in Fig. 1a. The chemical composition of HEAs and ADC12 alloy is shown in Table 1 and Table 2, respectively.

HEA powder was briquetted, cut into pellets and added to the melt. ADC12 ingot was firstly placed in an alumina crucible and melted in a resistance furnace at 750 $^{\circ}\text{C}$. Subsequently, the prepared HEAs pellets were added to the melt when the ingot had been completely melted. After that, the preheated ultrasonic probe was extended to the position 20 mm below the melt surface and ultrasound (900 W, 20 kHz) was applied for approximately 5 min. Finally, the melt was poured into a preheated steel mold (400 $^{\circ}\text{C}$) when the melt temperature dropped to 700 $^{\circ}\text{C}$. The matrix was cast by the

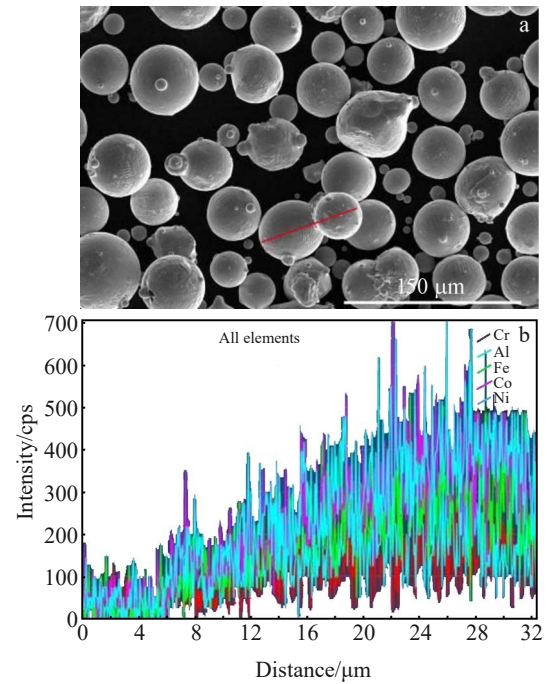


Fig.1 SEM image of AlCoCrFeNi HEAs (a) and EDS line scan spectra along red line in Fig.1a

Table 1 Chemical composition of AlCoCrFeNi HEAs (wt%)

Co	Cr	Fe	Ni	Al
24.97	21.34	23.55	24.54	Bal.

Table 2 Chemical composition of ADC12 alloy (wt%)

Cu	Fe	Si	Zn	Mg	Al
\leq 3.5	1.2-1.5	9-12	0.5	0.3	Bal.

same process with the same ultrasonic power and time for the comparison of microstructure as well as mechanical property.

Wear tests were carried out using a pin-on-steel disk tribometer^[30-31]. The wear test was carried out at a rotational speed of 100 r/min (0.188 m/s) at room temperature under 20 N. The disk friction pair was ASTM 1045 steel with a hardness of 55 HRC. The friction test samples were machined into pins with 4.5 mm in diameter by wire-cutting. All test materials had to be ultrasonically cleaned and dried prior to wear testing. In addition, the mass of each sample was measured before and after the wear test using a FA2204B electronic balance with an accuracy of 0.1 mg. Wear trace morphologies of typical samples were investigated by SEM.

The optical microstructures of the prepared composite samples were observed with an optical microscope (OM, Nikon ECLIPSE MA200) combined with SEM. The hardness of all samples was measured with a micro-Vickers hardness tester (HVS 1000A). Mechanical properties and strengthening effect were explored by tensile tests (Fig. 2) on a universal testing machine (TXYA 105C) at room temperature with displacement rate of 0.2 mm/min. All tests were repeated 9 times to ensure the accuracy of the values.

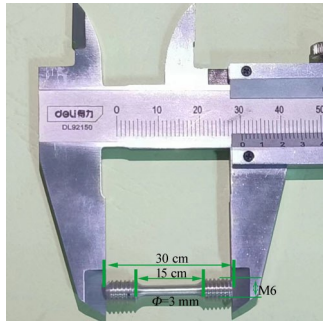


Fig.2 Tensile sample of the fabricated composite

2 Results and Discussion

2.1 Microstructure

In order to investigate the presence form of HEA particles in HEA/ADC12 composites, the element mappings analysis of ADC12 alloy containing 7wt% HEAs was carried out by transmission electron microscope (TEM) and EDS, as shown in Fig.3. It can be clearly seen that the elements belonging to the original HEAs, such as Fe, Co, Cr, Ni and Al elements, are in the same position in the matrix, which indicates that most of the elements are effectively preserved due to the desirable stability of the HEA particles, even after the high-intensity ultrasonic casting.

Fig.4a shows a representative TEM image of 7wt% HEAs/ADC12 composite. It can be seen that the HEAs added into the ADC12 matrix exhibit a clear blocky morphology, which is consistent with Fig.2. Fig.4b shows the HEA/Al interface morphology in the HEA/ADC12 composite. It can be seen that the HEAs are well bonded to the Al matrix without

defects such as microcracks and holes, indicating excellent interfacial bonding of HEAs with the aluminum matrix. It is possible that a small number of elements on the surface of the HEAs unavoidably react with the matrix to strengthen the interfacial bonding. In general, a good interfacial bonding between the reinforcement and the matrix is beneficial for the load transfer from the matrix to the reinforcement with higher strength^[32], which will ultimately be beneficial for the strength enhancement of the prepared composites. In addition, a large number of dislocation clusters appear around the HEA powder, which is due to the difference in thermal mismatch coefficients between the reinforcement and the matrix.

Typical microstructures of ADC12 alloys with various HEA contents are shown in Fig. 5. As shown in Fig. 5a, the microstructure of ADC12 alloy consists of primary aluminum, coarse plate-like or dendritic eutectic Si, granular Al_2Cu and trace $\beta\text{-Fe}$ phases (coarse needle-like $\beta\text{-Al}_3\text{FeSi}$)^[33]. The coarse Si phase, however, is a potential crack initiation point and leads to deterioration of mechanical properties^[34-36]. When 7wt% HEAs are added to the melt, the profile of the $\alpha\text{-Al}$ phase of the fabricated composites tends to be clear, and the coarse platelet Si phase shows a tendency to be refined. As shown in Fig.5c, the Si phase is completely modified into a fine fiber-like structure with the increase in the amount of HEAs to 12wt%. The $\alpha\text{-Al}$ grains are further refined. The secondary dendrite spacing decreases significantly. It can be inferred that the addition of HEAs significantly alters the eutectic Si phase. Meanwhile, combined with the deep corrosion morphologies of the composites (Fig. 6), it can be found that the Al_2Cu phase of elevated amount at the grain boundaries is accompanied by a granular appearance. These particles overlap with the refined Si phase. It is also worth

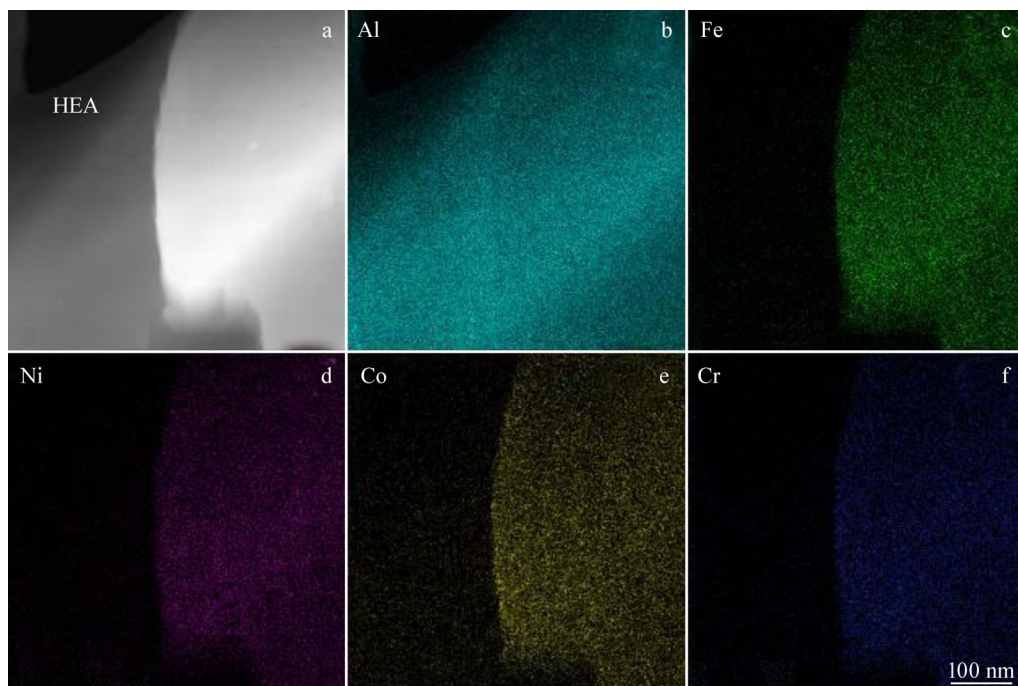


Fig.3 TEM image (a) and EDS element mappings (b-f) of HEAs in composites

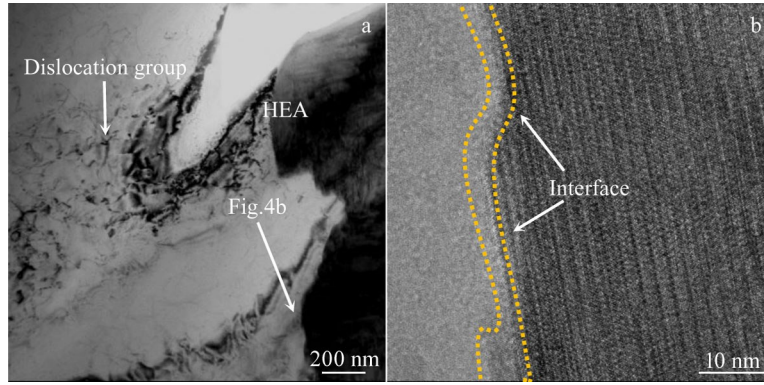


Fig.4 TEM images of morphology (a) and magnified interface (b) of 7wt% HEAs/ADC12 composites

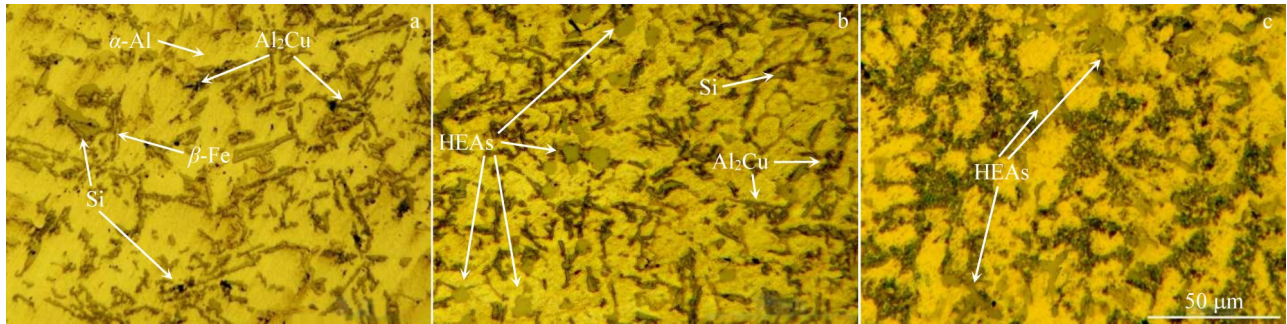


Fig.5 Microstructures of alloy with different HEA particles additions: (a) 0wt%, (b) 7wt%, and (c) 12wt%

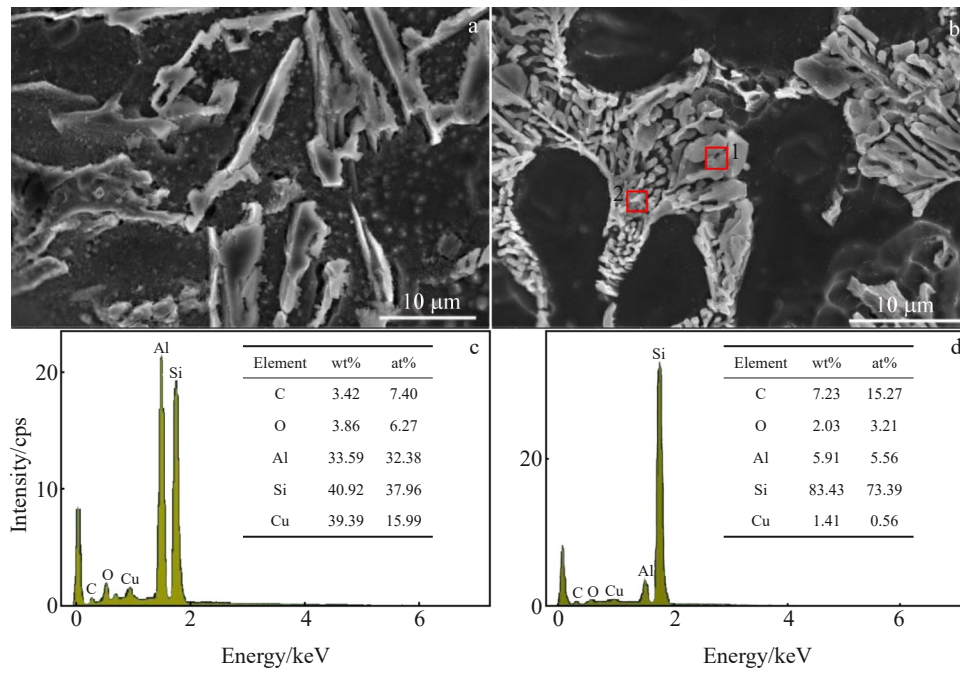


Fig.6 SEM images of ADC12 aluminum alloys free of HEAs (a) and with 12wt% HEAs (b); EDS results of area 1 (c) and area 2 (d) in Fig.6b

noting that are a small number of agglomerated phases of HEAs, as shown in Fig.5c.

2.2 Material properties

Fig. 7 shows the stress-strain curves and average Vickers hardness of the alloys containing different contents of HEAs, and the tensile properties are shown in Table 3. The ultimate

tensile strength (UTS), yield strength (YS) and elongation of the matrix are 185 MPa, 155.0 MPa and 2.47%, respectively. It is clear that the UTS and YS of the composite samples increase after the addition of HEAs. The UTS and YS of the composites increased to 219.0 MPa and 171.6 MPa, respectively, when the content of HEAs is 7wt%. In addition, the

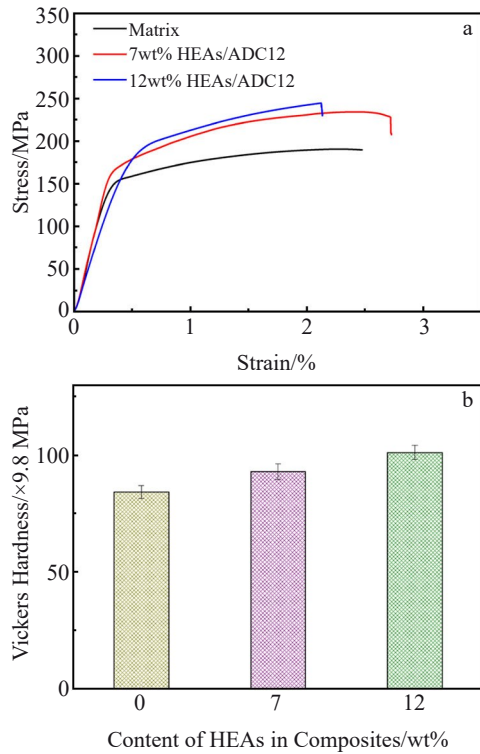


Fig.7 Tensile stress-tensile strain curves (a) and Vickers hardness (b) of composites with different contents of HEAs

Vickers hardness of the composites increases to 924.14 MPa compared to 799.68 MPa of the matrix, as shown in Fig. 7b. However, the change in elongation is small. With further increase in the content of HEAs in the composites to 12wt%, UTS as well as YS of the composites is further increased to 237 and 180 MPa, which are higher than those of the matrix alloy by 21.9% and 16.9%, respectively. The Vickers hardness of the prepared composites shows a similar increasing trend to 999.60 MPa. The mechanical properties are strengthened, which is related to the dislocation diffusion due to the addition of HEAs as well as the load transfer of the strengthened phases^[37].

2.3 Fractography

Fig. 8 illustrates the tensile fracture morphologies of the composites with different HEAs contents. Fig. 8a shows the fracture surface of as-cast ADC12 alloy, which is mainly composed of dimples and a few tear ribs. This indicates that ductile fracture is the primary mode of fracture for the matrix sample. As shown in Fig. 8b, after the addition of 7wt% HEAs to the alloy, a large number of dimples remain on the fracture surface of the composite sample. This indicates that the fracture mode of the sample is still dominated by ductile

fracture. In addition, some plate-like particles are found in the larger dimples, which are confirmed as the added HEAs by EDS. This phenomenon indicates that part of the load carrying capacity of the sample has been successfully transferred from the matrix to the reinforcement during the tensile test due to the good interfacial bonding. As shown in Fig. 8c, it can be observed that the tearing surfaces as well as brittle flat surface appear along with the presence of dimples after addition of 12wt% HEAs to the alloy. At the same time, the size and the number of dimples show a decreasing trend. This corresponds to the slight decrease in the elongation during the tensile test.

2.4 Wear properties

Fig. 9 and Fig. 10 exhibit the worn surfaces and coefficients of friction of the matrix and composites under applied load of 20 N, respectively. During dry sliding friction, different bearing materials exhibit different forms of wear. As shown in Fig. 9, there are distinctive smooth streaks and peeling pits on the worn surface of the matrix. Severe oxide stripping and plastic deformation occur during friction process due to the low hardness. When 7wt% HEAs are added to the alloy, a small number of grooves appear on the surface of the composites. It can also be noticed that the delamination on the surface is reduced. The width of the plastic zone also decreases. This indicates that the wear mechanism of the composites has changed and is dominated by abrasive wear. As the HEA particles content in the composites increases to 12wt% , the plastic deformation bright zones on the worn surface of the composites are hardly visible. Instead, a large number of scraped grooves appear on the worn surface, as shown in Fig. 9c. Although delamination is still present on the wear surface, the width of the delamination pits decreases significantly. It illustrates that the wear resistance of the composite is improved due to the addition of HEA particles.

The average wear rates of the test samples are exhibited in Fig. 10d. Fig. 10a–10c show typical variation of coefficient of friction (COF) with sliding time. The average COF and wear rate of ADC12 alloy free of HEAs are 0.350 and $22.7 \times 10^{-3} \text{ mm}^3/\text{m}$, respectively. After the addition of HEA particles, the COF and wear rate of composites are significantly decreased. The average COF and wear rate of 7wt% HEAs/ADC12 composite decrease to 0.317 and $19.4 \times 10^{-3} \text{ mm}^3/\text{m}$, respectively. Furthermore, both average COF and wear rate decrease to 0.289 and $15.8 \times 10^{-3} \text{ mm}^3/\text{m}$, respectively, when the content of HEA particles increases to 12wt%, which are much lower than those of the matrix. However, inevitably, the smoothness of friction decreases more significantly, which indicates an increase in the surface hardness of the composites, as previously described.

Table 3 Tensile properties of composites with different contents of HEAs

Material	YS/MPa	UTS/MPa	Elongation/%
ADC12	155.0±5.26	185±4.82	2.47±0.27
7wt% HEAs/ADC12	171.6±3.42	219±3.20	2.75±0.23
12wt% HEAs/ADC12	180.0±4.40	237±4.20	2.13±0.14

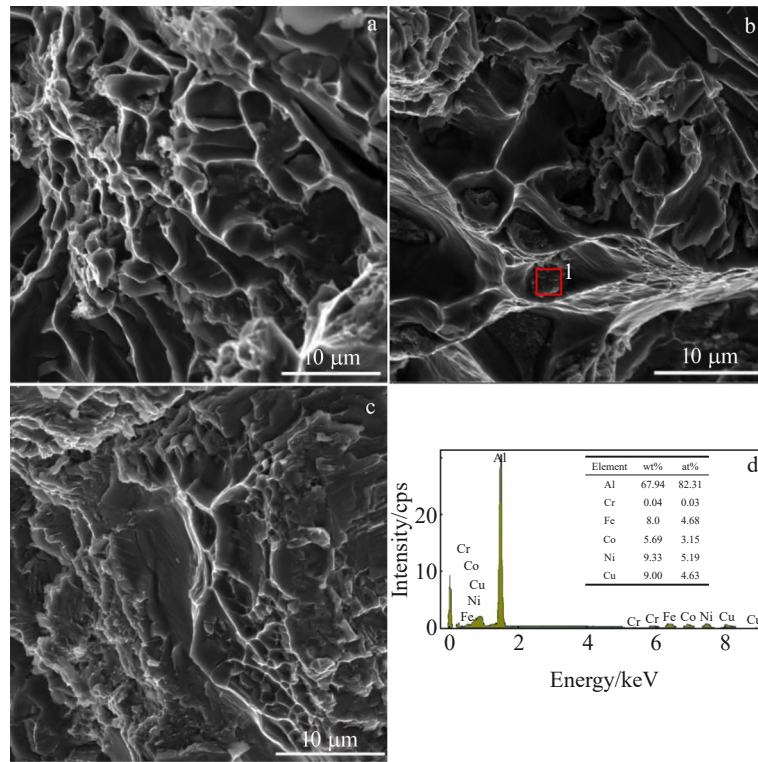


Fig.8 Fracture morphologies of ADC12 alloy (a), 7wt% HEAs/ADC12 composite (b), and 12wt% HEAs/ADC12 composite (c); EDS results of area 1 in Fig.8b (d)

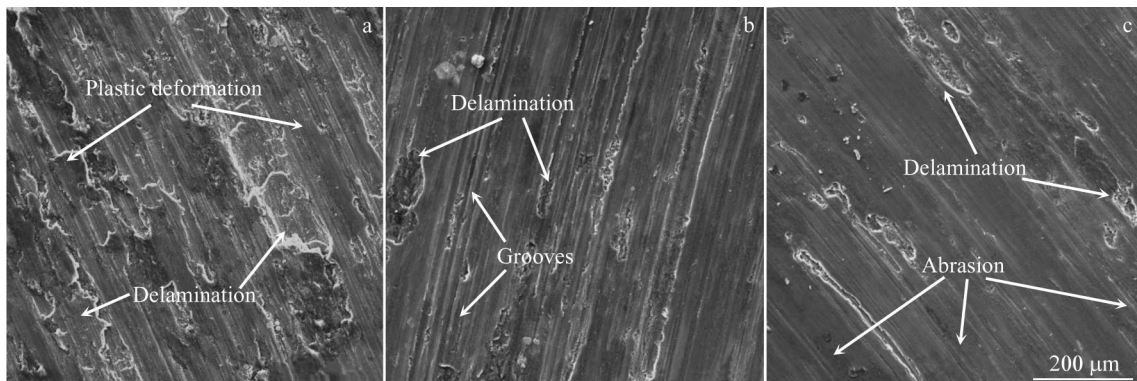


Fig.9 SEM morphologies of worn surfaces for as-cast ADC12 alloy (a), 7wt% HEAs/ADC12 composite (b), and 12wt% HEAs/ADC12 composite (c)

3 Discussion

The theoretical YS enhancement values of composites due to the addition of HEAs can be analyzed by two main enhancement mechanisms, which are considered to be load transfer strengthening and dislocation strengthening.

(1) Load transfer strengthening. External loads are transferred from the matrix to the reinforcement via interfacial shear stresses, which contribute to the reinforcement to assume loads in tension or compression state of the alloy. This strengthening mechanism should be based on excellent interfacial bond between the HEA particles and the matrix. The incremental expression for the contribution of this

mechanism to the YS of the composite can be calculated by the following equation^[38]:

$$\Delta\sigma_{LT} = \frac{f_v}{2} \sigma_m \quad (1)$$

where $\Delta\sigma_{LT}$ is the increment value of yield strength, f_v is the volume fraction and σ_m is the YS of the matrix. Here, YS of the matrix is equal to 154 MPa. Based on volume-to-mass conversion, 3.9vol%–6.3vol% HEAs can be obtained. Thus, the theoretically calculated value is 2.96–4.8 MPa.

(2) Dislocation strengthening. Dislocation strengthening is considered to be another important strengthening mechanism in composites that cannot be ignored. The variability in the coefficient of thermal expansion between the matrix material

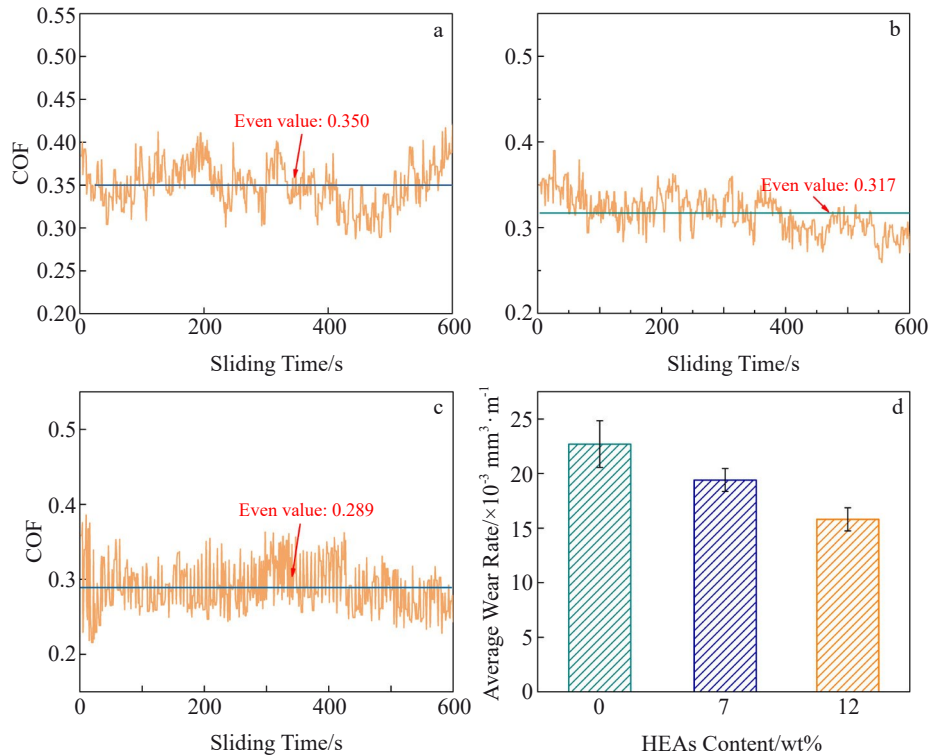


Fig.10 Transient COF (a–c) and average wear rate (d) of the composites with different HEAs contents under 20 N: (a) HEAs-free, (b) 7wt%, and (c) 12wt%

and HEAs leads to a large number of dislocations in the composite, as shown in Fig.11. The interaction of dislocations, such as the accumulation of plugs and tangles, acts as an obstacle to plastic deformation. Therefore, the presence of such dislocations strengthens the mechanical properties of the composite in turn^[38–40]. This is one of the main reasons for the increase in microhardness of fabricated composites.

$$\sigma_{\text{CET}} = 1.25Gb \sqrt{\frac{12\Delta T\Delta C f_v}{bd_p}} \quad (2)$$

where G and b are shear modulus of the matrix (Al) and the value of Burgers vector (0.286 nm), respectively; ΔT and ΔC represent the difference between the preparation temperature (720 °C) and room temperature (20 °C) and the difference in coefficient of thermal expansion, respectively; d_p is the

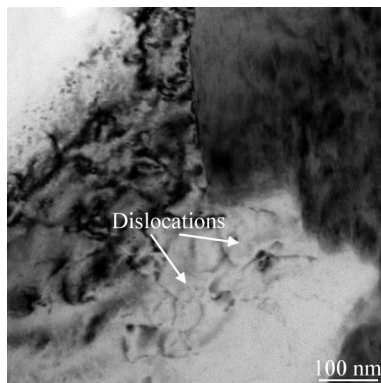


Fig.11 HRTEM image of dislocations in composites

equivalent diameter of HEAs. The theoretically YS value calculated by Eq.(2) increases to 21.2–27.0 MPa.

As can be seen from the current calculations, the YS values of the actually measured values show a small deviation from the sum of theoretical values of YS obtained by the two strengthening mechanisms. The small deviation of the values is mainly due to two reasons: the inevitable HEAs fragmentation due to high energy sonication as well as atomic diffusion^[41] after the addition of HEAs to the melt. This enhances the bonding at the HEA/Al interface. However, this may also lead to inaccuracy in the size of some HEAs, as well as uncertainty in the composition of the generated phases in the vicinity of HEAs. Moreover, the increase in the theoretically calculated YS value should be based on a uniform distribution of all reinforcement particles. As a result, the actual YS increments of the prepared composites deviate from the theoretically calculated values.

In addition, it is found that the wear resistance of the prepared composites is enhanced. The resistance to plastic deformation of fabricated composites is improved, as shown in Fig. 10. The plastic deformation zones decrease with the addition of HEAs. This can be attributed to two reasons. The increased microhardness is due to the high hardness of HEA itself and dislocation proliferation. The Vickers hardness value of the composite with 12wt% HEAs increases from 799.68 MPa to 999.60 MPa, increased by 25%. The increase in Vickers hardness of the composites directly restricts the plastic deformation of the sample during friction^[42–43]. In addition, the refinement and uniform distribution of Al_2Cu or

Si phase further enhance the resistance to plastic deformation. Thus, it ultimately contributes to the reduction in the wear rate of the HEAs/ADC12 composites.

4 Conclusions

1) After the addition of HEAs to the ADC12 melt, the α -Al dendrites are refined. The bulk Si phase as well as the Al_2Cu phase shows granular distribution at the grain boundaries.

2) The UTS and YS of 12wt% HEAs/ADC12 composites are 237 and 180.0 MPa, which are higher than those of the matrix alloy by 21.9% and 16.9%, respectively. Accordingly, the microhardness of the composite is 999.60 MPa, which is 25% higher than that of the matrix.

3) The addition of HEAs results in a significant increase in the abrasion resistance and a decrease in the COF. The COF and the wear rate decrease from 0.350 and $22.7 \times 10^{-3} \text{ mm}^3/\text{m}$ of composites without HEAs to 0.289 and $15.8 \times 10^{-3} \text{ mm}^3/\text{m}$ of composites with 12wt% HEAs.

4) The improvement in the mechanical properties of the composites can be attributed to the dislocation proliferation, load transfer mechanism and optimization of the microstructure.

References

- Zeng F, Meng Z, Guo W. *Materials Letters*[J], 2022, 306: 130807
- Sun C, Li H, Shcheretskyi H V. *International Journal of Metalcasting*[J], 2024, 18(1): 457
- Zhao Y L, Bian L P, Zhao X G et al. *Rare Metal Materials and Engineering*[J], 2019, 48(7): 2165
- Chen Kanghua, Fang Huachan, Zhang Zhuo et al. *Rare Metal Materials and Engineering*[J], 2009, 38(4): 607 (in Chinese)
- Santhosh P A, Parameshwaran P T. *Industrial Lubrication and Tribology*[J], 2023, 75(2): 204
- Anbucheziyan G, Shanmugam V, Vignesh M et al. *Materials Letters*[J], 2024, 357(15): 1
- Qin Y N, Wang Y Z, Wen H B et al. *Materials Science Forum*[J], 2023, 1080: 41
- Guo R F, Chen S M, Shen P. *Journal of Materials Research and Technology*[J], 2023, 27(11): 6104
- Xu R, Li R, Yuan T et al. *Acta Metallurgica Sinica (English Letters)*[J], 2022, 35(3): 411
- Lee D, Kim J, Park B et al. *Metals*[J], 2021, 11(3): 413
- Lv Z Z, Liu X, Wang J et al. *Materials Letters*[J], 2023, 334: 133728
- Prasad D S, Shoba C. *Journal of Materials Research and Technology*[J], 2014, 3(1): 79
- Enel M, Gürbüz. *Archives of Metallurgy and Materials*[J], 2021, 66(1): 97
- Mordyuk B, Prokopenko G, Milman Y et al. *Materials Science and Engineering A*[J], 2013, 563: 138
- Hou J, Chi F, Chi L et al. *Journal of Alloys and Compounds*[J], 2022, 902: 162538
- Ertugrul O, He T B, Shahid R N et al. *Journal of Alloys and Compounds*[J], 2019, 808: 151732
- Yu P, Zhang L C, Zhang W Y et al. *Materials Science and Engineering A*[J], 2007, 444: 206
- Liu Y Z, Chen J, Li Z et al. *Journal of Alloys and Compounds*[J], 2018, 780(5): 558
- Wang Z W, Yuan Y B, Zheng R X et al. *Transactions of Nonferrous Metals Society of China*[J], 2014, 24(7): 2366
- Wang H M, Ren W X, Li G R et al. *Materials Science and Engineering A*[J], 2021, 801: 140406
- Liu Y, Chen J, Li Z et al. *Journal of Alloys and Compounds*[J], 2019, 780: 558
- Yuan Z W, Tian W B, Li F G et al. *Journal of Alloys and Compounds*[J], 2019, 806: 901
- Chen W P, Li Z X, Lu T W et al. *Materials Science and Engineering A*[J], 2019, 762: 138116
- Mohan R M, Kempaiah U N, Manjunatha B et al. *Materials Physics and Mechanics*[J], 2022, 50(2): 304
- Rajeswari B, Manikandan C. *Materials Today: Proceedings*[J], 2023, 4(6): 406
- Ramachandran M, Thirunavukarasu K, Pramod V R. *International Journal of Engineering Trends and Technology*[J], 2021, 69(3): 103
- Liu N, Jiang B, Ji Z et al. *Modern Physics Letters B*[J], 2022, 36(4): 2150571
- Mohan R M, Kempaiah U N, Manjunatha B et al. *Materials Physics and Mechanics*[J], 2022, 50(2): 304
- He C, Wei J, Li Y et al. *Journal of Materials Science and Technology*[J], 2023, 133: 183
- Hu Y, Zheng, Y, Politis, D J et al. *Tribology International*[J], 2019, 130: 216
- Wu Q J, Yan H, Zhang P X et al. *Acta Metallurgica Sinica*[J], 2018, 31(5): 523
- Wan X J, Lin J G. *Transactions of Nonferrous Metals Society of China*[J], 2011, 21(5): 1023
- Rao Y Y, Hong Yan, Zhi H. *Journal of Rare Earths*[J], 2013, 31(9): 916
- Shin S S, Kim E S, Yeom G Y et al. *Materials Science & Engineering A*[J], 2012, 532(1): 151
- Shabestari S G, Parshizfard E. *Journal of Alloys and Compounds*[J], 2011, 509(30): 7973
- Huang Z X, Yan H, Wang Z W. *Journal of Central South University*[J], 2018, 25(6): 1263
- Xiao Y, Peng D, Zhifeng Y et al. *Journal of Alloys and Compounds*[J], 2020, 836: 155411
- Yuan Q H, Qiu Z Q, Zhou G H et al. *Materials Characterization*[J], 2018, 138: 215
- Jiang L, Yang H, Yee J et al. *Acta Materialia*[J], 2016, 103(15): 128
- Yuan Q H, Zheng X S, Wang Y C et al. *Journal of Materials*

- Science & Technology[J], 2017, 33(5): 452
- 41 Meng G H, Lin X, Xie H et al. *Journal of Alloys and Compounds*[J], 2016, 672(5): 660
- 42 Mazahery, Ali S, Mohsen O. *Transactions of Nonferrous Metals Society of China*[J], 2013, 23(7): 1905
- 43 Chen C C, Chen G, Yan H G et al. *The Chinese Journal of Nonferrous Metals*[J], 2011, 21(6): 1258

高熵合金 AlCoCrFeNi 对 Al-Si-Cu 合金微观结构和力学性能的影响

吴庆捷¹, 郭正华¹, 黄勤², 凌李石保³

(1. 南昌航空大学 航空制造工程学院, 江西 南昌 330036)

(2. 江西五十铃汽车有限公司 技术研发部, 江西 南昌 330010)

(3. 嘉善鑫海精密铸造有限公司, 浙江 嘉兴 314101)

摘要: 高熵合金 (HEA) AlCoCrFeNi 作为一类新型合金材料, 具有高稳定性、优异的比强度和耐腐蚀性等特点, 在铝基复合材料 (AMC) 领域备受关注。为了研究 AlCoCrFeNi HEA 颗粒对铝合金微观结构和力学性能的影响, 采用高能超声铸造工艺制备了 AlCoCrFeNi HEA 颗粒增强 ADC12 复合材料。随后, 研究了添加 HEA 对 ADC12 合金微观结构和力学性能的影响。结果表明, 添加的 HEA 颗粒与铝基体紧密结合。基体中的 Al₂Cu 以及硅相得到了细化。同时, 添加了 HEA 颗粒的合金抗拉伸强度和显微硬度得到了显著提高。与基体相比, 含 12% (质量分数) HEA 复合材料的屈服强度和极限拉伸强度分别提高了 16.9% 和 21.9%。在 20 N 载荷下, 复合材料的磨损率也因显微硬度的提高而降低, 这主要归因于载荷传递强化、位错增殖和显微结构优化。

关键词: 高熵合金 (HEA); ADC12 铝合金; 铝基复合材料 (AMC); 力学性能

作者简介: 吴庆捷, 男, 1985 年生, 博士, 南昌航空大学航空制造工程学院, 江西 南昌 330036, 电话: 0791-83863028, E-mail: wu856200@163.com